Talanta 217 (2020) 121063

Contents lists available at ScienceDirect

Talanta

journal homepage: www.elsevier.com/locate/talanta

Fast construction of polymer monolithic columns inside fluorinated ethylene propylene (FEP) tubes for separation of proteins by reversed-phase liquid chromatography

Fernando H. do Nascimento, Amanda H. Moraes, Catharina R.L. Trazzi, Caryna M. Velasques, Jorge C. Masini*

Departamento de Química Fundamental, Instituto de Química, Universidade de São Paulo, Av. Prof. Lineu Prestes 748, 05508-000, São Paulo, SP, Brazil

ARTICLE INFO

Keywords:
Fluoropolymer tubes
Photografting
Monolithic columns
Liquid chromatography
Urine
Egg white

ABSTRACT

This paper describes the preparation of polymer monolithic columns in the confines of fluorinated ethylene propylene (FEP) tubes. These tubes are cheap, chemically stable, and widely used in flow analysis laboratories. UV-initiated grafting with 5 wt% benzophenone in methanol for 1 h activated the internal surface walls, thus enabling the further covalent binding of ethylene glycol dimethacrylate (EDMA) from a 15 wt% solution in methanol, also via photografting. Both steps used 254 nm radiation under a potency of 120 mJ cm^2. ATR-FTIR measurements revealed the presence of carbonyl, alkyl and vinyl groups in the functionalized FEP. The density of vinyl groups was high enough to firmly attach a poly(lauryl methacrylate-*co*-ethylene glycol dimethacrylate) monolith in 120 × 1.57 mm i.d. tubes, prepared via photopolymerization. The total preparation lasts less than 2-h. The columns were permeable, (1.58 ± 0.06) × 10^{-13} m^2, providing reproducible chromatographic parameters of retention times, retention factor, selectivity, and resolution. The monoliths were stable at flow rates of 500 μL min^{-1}, collapsing only at flow rates > 700 μL min^{-1}, a condition that increased the backpressure over 1000 psi (experiments at the room temperature). The separation of proteins by reversed-phase liquid chromatography demonstrated the efficiency of the columns. Determination of egg white proteins (ovalbumin and lysozyme) and myoglobin in spiked urine proved the applicability to the analysis of real samples.

1. Introduction

Polymeric monolithic columns have been useful tools in proteomics [1,2] by providing efficient separation of intact proteins [3] and versatile platforms for the construction of immobilized enzymatic reactors [4,5]. In their beginning, the monoliths were prepared by free radical thermal polymerization inside inox tubes having internal diameters of 4.6–8.0 mm, which enabled the fast separation of proteins at high flow rates [6]. The growing demand for hyphenation of liquid chromatography with mass spectrometers motivated the miniaturization of the columns [7,8]. Currently, most of the polymer monoliths are prepared in fused silica capillaries (i.d. < 100 μm), requiring a drastic reduction of the extra-column volumes to avoid a significant decrease in sensitivity, since the sample volumes also have to be dramatically reduced [7,9,10].

Currently, there is a keen interest in the narrow bore and semi-micro columns (0.50–2.0 mm i.d.) to fill the gap between the regular columns (4.6 mm i.d.) and the capillaries (< 100 μm i.d.) [7,11]. Polymer monoliths in such intermediate dimensions were prepared inside activated polyetheretherketone (PEEK) [12,13], or fused silica lined stainless steel tubes [14,15]. These tubes were first activated by grafting a thin layer of poly(EDMA) in the case of PEEK or 3-(trimethoxysilyl)propyl methacrylate in fused silica. The in-situ thermally-assisted polymerization was simultaneous with the covalent bonding of the monoliths to the pendant vinyl groups grafted at the inner walls of the activated tubes.

Photo-polymerization is an attractive approach for the fast construction of polymeric monoliths. While thermal polymerization takes several hours to achieve acceptable reaction extension, photo-polymerization requires only a few minutes [16]. However, mechanically resistant UV-transparent tubes (PTFE-coated fused silica) are commercially available only in the capillary dimensions (o.d. 363 ± 10 μm × 50–100 μm i.d.). The construction of 0.50–2.0 mm i.d. columns by photopolymerization motivated investigations on the viability of using polypropylene (PP) and fluoropolymer tubes [16–18]. PP houses monolithic phases for SPE inside pipette tips, syringes barrels,

* Corresponding author.
E-mail address: jcmasini@iq.usp.br (J.C. Masini).

https://doi.org/10.1016/j.talanta.2020.121063
Received 12 February 2020; Received in revised form 15 April 2020; Accepted 17 April 2020
Available online 20 April 2020
0039-9140/

syringe filters, etc. [19,20]. In these cases, the restrictions imposed by the conical format of pipette tips, or by the end restriction of syringes, assured the monoliths were held inside the housing. However, channeling may appear in the interface between the polymer and the tube wall, reducing the retention. Stachowiak et al. [21] circumvented this issue in a pioneering method featuring a UV-initiated reaction mediated by benzophenone (BP). First, the internal walls of PP micropipette tips were photografted with a thin interlayer of a polymer affording a multiplicity of pendant double bonds to support the monolith. This approach was explored to prepare SPE cartridges inside syringe barrels using BP for proton abstraction, followed by the second step of modification with EDMA to vinylize the internal surface for the further covalent attachment of the monolith [22].

Using the two-step photografting with BP and EDMA, Catalá-Icardo et al. prepared poly(glycidyl methacrylate-*co*-divinylbenzene), poly (butyl methacrylate-*co*-ethyleneglycol dimethacrylate) and poly (styrene-*co*-divinylbenzene) monoliths inside poly(ethylene-*co*-tetrafluoroethylene) (ETFE) tubing with internal diameters of 0.75 and 1.50 mm for reversed-phase separation of alkylbenzenes and proteins. The polymerizations were thermally assisted for 8 h [17]. In another work, after the two-step photografting of the 0.75 mm i.d. ETFE tubing, the authors studied the influence of the free-radical initiators α,α′-azobisisobutyronitrile (AIBN), 2,2-dimethoxy-2-phenyl acetophenone (DMPA) and 2-methyl-40-(methylthio)-2-morpholinopropiophenone (MTMPP) for the photo-assisted polymerization of poly(butyl methacrylate-*co*-ethylene glycol dimethacrylate) monolith [18]. The columns separated mixtures of alkylbenzenes, intact proteins, protein digests, and phenyl urea herbicides by reversed-phase liquid chromatography (RPLC) [18].

Fluorinated ethylene propylene (FEP) tubes are widely available in laboratories. They are UV-transparent and have excellent chemical and mechanical stability. Differently from ETFE, FEP has only C–C and C–F bonds, with no abstractable hydrogen, thus requiring drastic treatment for photografting. For instance, Noh et al. [23] photografted PTFE with benzophenone in the presence of a strong reducing agent (sodium hydride) in dry dimethylformamide.

In the present paper, we demonstrated for the first time that FEP tubes could be photografted with BP only by just increasing the radiation time. After the first activation step with BP the internal surface can be easily functionalized with EDMA following the procedures already described by either Iacono et al. [16] or Catalá-Icardo et al. [17]. The density of vinyl groups was enough to hold a poly(lauryl methacrylate-*co*-ethyleneglycol dimethacrylate), poly(LMA-*co*-EDMA), monolith prepared by photopolymerization inside 120 × 1.57 mm i.d. tubes at backpressures up to 1000 psi. Determination of lysozyme and ovalbumin in egg white and myoglobin in urine demonstrated the applicability of the columns to the analyzes of real samples.

2. Experimental

2.1. Reagents

Lauryl methacrylate (LMA) and ethylene glycol dimethacrylate (EDMA) were obtained from Sigma-Aldrich (St. Louis, MO, USA) and purified by passing them through an basic aluminum oxide column for removal of polymerization inhibitors. 1-Propanol, 1,4-butanediol (porogenic solvents), benzophenone (BP) and 2,2-dimethoxy-2-phenyl acetophenone (DMPAP) were purchased from Sigma Aldrich and used as received. Methanol, acetone, and ethyl alcohol were of analytical grade from Sigma-Aldrich. HPLC grade acetonitrile from J.T. Baker (Avantor Performance Materials, PA, USA) and trifluoroacetic acid (TFA, Sigma-Aldrich) was used in the preparation of the mobile phases. KH_2PO_4, and K_2HPO_4 used for the preparation of phosphate buffer solution (PBS) were analytical grade reagents from Merck. Lysozyme and ovalbumin from chicken eggs, ribonuclease A from bovine pancreas, and myoglobin from horse skeleton muscle were from Sigma-Aldrich. These proteins were dissolved in water (0.5–1.0 mg mL^{-1}), and filtered through 0.45 μm cellulose acetate syringe filters before the chromatographic analyses. Deionized water (resistivity > 18 MΩ cm) from a Simplicity 185 system from Millipore (Billerica, MA, USA) was used for the preparation of solutions. Fluorinated ethylene propylene (FEP) 1.57 mm i.d. × 3.18 mm o.d. tubing from IDEX Health & Science housed the columns.

2.2. Instrumentation

Chromatographic analyses were made in a Dionex Ultimate 3000 Dual Micro LC system (Dionex Softron GmbH, ThermoFisher Scientific, Germany) using dual micro DGP-3600 RS pumps with an SRD-3600 in-line degasser, provided with a WPS-3000SL automatic sampler and a sampling loop for volumes between 0.1 and 20 μL. A TCC 3000SD thermostated column compartment and an MWD-3000 UV/Vis detector coupled to a 2.5 μL semi-micro flow cell completed the chromatographic system. Control of the instrument, data acquisition, and data processing was made with the software Chromeleon® 6.8. Connections of the column tube to the analyzers were made with P-702 PEEK unions, XP-335 PEEK nuts and P-300 ETFE ferrules from IDEX Health and Science (Oak Harbor, WA, USA).

Photografting and photo-polymerization were made in a Specrolinker XL-1000 UV-crosslinker from Spectronics Corporation (Westbury, New York, USA) provided with five 8-W, 254 nm lamps.

Washing of the columns with acetonitrile or water was made with Shimadzu LC-9 (Shimadzu, Japan) pumps. Scanning electron microscopy (SEM) was made with a Fesem Jeol JSM -740 1 F instrument (Jeol Ltda, Tokyo, Japan). Attenuated total reflectance Fourier Transform Infrared Spectroscopy (ATR-FTIR) spectra of the inner wall of the FEP tubes were obtained from 540 to 4000 cm^{-1} in a Frontier FT-IR instrument from PerkinElmer (Waltham, MA, USA).

2.3. Functionalization of the inner wall of the FEP tubes

150-mm long FEP tubes were washed with ethanol and acetone (five times with 1 mL aliquots of each solvent) and dried under N_2. A 5 wt% solution of BP in methanol was sonicated (10 min) and purged with N_2 (10 min). Then, this solution was used to fill the tubes, which were closed in both ends and irradiated for 60 min under 254 nm at 120 mJ cm^{-2}. The tubes were positioned 2.5 cm apart from the UV-lamps, and a rigid plastic plate covered with reflexive aluminum foil was placed just behind the columns. After this first step, the tubes were washed with methanol, dried with N_2, and filled with a 15 wt% solution of EDMA in methanol, previously sonicated (10 min), and purged with N_2 (10 min). The tubes were then closed in both ends and irradiated for 20 min under 254 nm at 120 mJ cm^{-2}, keeping a distance of 2.5 cm apart from the lamps and the reflexive surface behind the columns. All the reactions were made with the photo-reactor in the vertical position. Finally, the tubes were washed with methanol and dried under a flow of N_2.

2.4. Preparation of the monoliths

A polymerization mixture containing 24 wt% LMA, 16 wt% EDMA, 45.5 wt% 1-propanol, and 14.5 wt% 1,4 butanediol [24] was prepared in a 2-mL amber vial in the presence of 1.0 wt% DMAP (relative to the monomers). The mixture was sonicated for 10 min and bubbled with N_2 for another 10 min. The activated FEP tubes were filled with the polymerization mixtures, closed in both ends, and irradiated for 20 min under 254 nm at 120 mJ cm^{-2} as in the activation procedures. Both column ends were cut to provide 120 mm long columns, which were then flushed with ACN at 500 μL min^{-1} until a constant pressure.

2.5. Samples

Egg white sample was diluted (1:1) in 0.050 mol L^{-1} PBS (pH 7.0) and centrifuged at 4000 × *g* for 15 min [25]. The resulting supernatant was filtered in 0.45 μm syringe filters and diluted in the PBS at 1:10 or 1:500 volumetric ratios and analyzed. Both solutions were then spiked with a mixture of lysozyme and ovalbumin to estimate the accuracy of the analysis via spiking/recovery experiments.

Urine samples were collected from one of the co-authors before and 10 min after physical exercises consisting of anaerobic strength training (1 h) followed by running (40 min). The samples were diluted (1:4) in 10 mmol L^{-1} PBS (pH 7.0) and filtered through 0.22 μm syringe filters [26]. The samples were then analyzed by the RPLC method before and after spiking with known concentrations of myoglobin.

3. Results and discussion

3.1. Functionalization of the FEP tubes

In principle, the photografting of the FEP tube is challenging because, differently of the ETFE tubes, FEP has no C–H bonds for H-abstraction by BP [17]. The ATR-FTIR of the pristine FEP tube confirmed the C–F bending band at 680 - 780 cm^{-1}, the -C-C- stretching in the side-chain C-CF_3 at 980 cm^{-1}, the two intense peaks at 1148 and 1203 cm^{-1} due to the CF_2 and CF_3 vibrations, as well as the band at 2370 cm^{-1} due to CF_2 stretching [27,28] (Fig. 1). The two low-intensity peaks at 2852 and 2930 cm^{-1} may be attributed to C–H stretching due to some FEP impurity (inset of Fig. 1). One-hour of photografting with BP led to the appearance of a typical wide O–H stretching band at 3423 cm^{-1}, which resulted from the reaction of the diphenyl ketyl intermediate with the FEP surface. Additionally, an absorption centered at 1628 cm^{-1} due to aromatic C=C confirmed the unsaturation of the surface of FEP after the grafting of BP (inset of Fig. 1).

Noh et al. [23] exposed PTFE surface to UV-radiation in the presence BP dissolved in dry DMF containing sodium hydride under inert atmosphere (N_2). They observed that 5-min of UV exposure caused significant defluorination, and the simultaneous incorporation of O. X-ray Photoelectron Spectroscopy (XPS) demonstrated that after 20 min of UV radiation, the content of F decayed from 68.44 to 7.30 wt%. In contrast, the O content increased from 0 to 20.69 wt%. The XPS measurements also observed significant surface unsaturation. All these findings were consistent with our observations by ATR-FTIR, with the difference that due to the softer chemical conditions used, the photografting of BP was observable only after 1 h of UV exposition. The presence of impurities containing C–H bonds cannot be ruled out (inset of Fig. 1), since previous XPS measurements of virgin FEP surfaces exhibited C–H peaks at 285 eV [28]. The weak intensity of the ATR bands in our work suggests a low density of grafted BP molecules. Early experiments using 20 min of UV radiation produced too few anchoring points so that the monoliths were expelled from the tubes as soon as the washing with acetonitrile started.

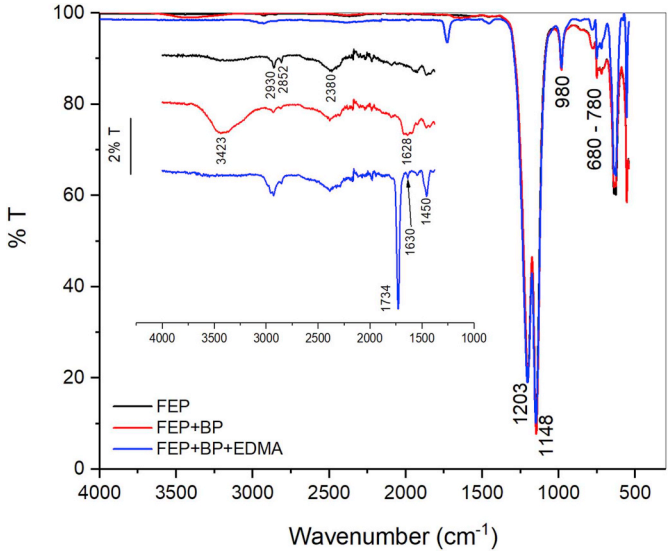

Fig. 1. ATR-FTIR of the inner wall of the FEP tube before (FEP) and after the photografting with BP (FEP + BP) and EDMA (FEP + BP + EDMA).

The photografting of EDMA was made for only 20 min, as described in the previously published papers [16,18]. The ATR spectrum shows the disappearance of the bands centered at 3423 cm^{-1} and 1628 cm^{-1}, remaining a small and narrower band at 1630 cm^{-1}, which corresponds to C=C stretching vibrations of the grafted poly(EDMA) (Fig. 1). The appearance of the peak at 1456 cm^{-1} due to the C–H bending of methyl groups, the increase of the intensity of the peaks at 2852 and 2930 cm^{-1} due to C–H stretching, and a more intense band at 1734 cm^{-1} due to the stretching of C=O bonds of the carbonyl groups of EDMA (Fig. 1) confirmed the grafting of EDMA. Although not determined, the density of vinyl groups created in the FEP tube is probably much lower than that in ETFE. Even so, 60 min of photografting with BP and 20 min with EDMA produced tubes whose internal surface firmly attached the monoliths.

The maximum flow rate and pressure supported by the columns were verified by pumping a mobile phase composed of 50:50 (v v^{-1}) ACN: H_2O at the ambient temperature without any physical restriction at the column end. The backpressure increased linearly with the flow rate until 700 μL min^{-1}, reaching about 1000 psi (Fig. S1). At this point, some collapse occurred, and the pressure dropped to about 700 psi at the flow rate of 800 μL min^{-1}. Then, the linearity was lost, and after an abrupt pressure rise to about 1400 psi (1600 μL min^{-1}), the mobile phase expelled the monolith from the tube. Thus, in the following work, the maximum flow rate was limited to 500 μL min^{-1}, heating the column compartment at 50 or 60 °C, a condition that kept the backpressure at about 400 psi.

3.2. Scanning electron microscopy

The photografting of the FEP tube with BP did not cause any visible alterations in the SEM images. After the photografting with EDMA, it is possible to observe an increase in the roughness of the internal surface of the tubes in comparison with the untreated tube (Fig. 2a and b). The cross-section of the column shows the monolith adhered to the poly (EDMA) interlayer (between the tube wall and the monolith) and the absence of gaps between the inner wall and the polymer (Fig. 2c). Installation and de-installation of the columns in the chromatograph cause some momentary bending in the flexible FEP tubes. Since the SEM images were acquired after several chromatographic uses of the column, it is clear that these small bendings do not prejudice the adherence of the polymers to the tube walls. The monoliths exhibited a quite regular distribution of globules with a mean diameter around 3 μm and flow-through pores of similar sizes (Fig. 2d and e). The large flow-through pores conferred high permeability for the columns.

3.3. Permeability and chromatographic performance

Five columns were prepared in two different working days using different lots of polymerization mixtures. This experiment aimed at the evaluation of the repeatability of the tube activation and polymerization procedures. The high permeability of (1.58 ± 0.06) × 10^{-13} m^2 enabled flowrates of 500 μL min^{-1} at backpressures < 500 psi, which is the recommended maximum pressure for FEP tubes having 1.57 mm i.d. (0.805 mm thick wall). The relative standard deviation of the permeabilities was 3.8%, thus denoting the excellent repeatability of the entire process of tube grafting and polymerization (Table S1).

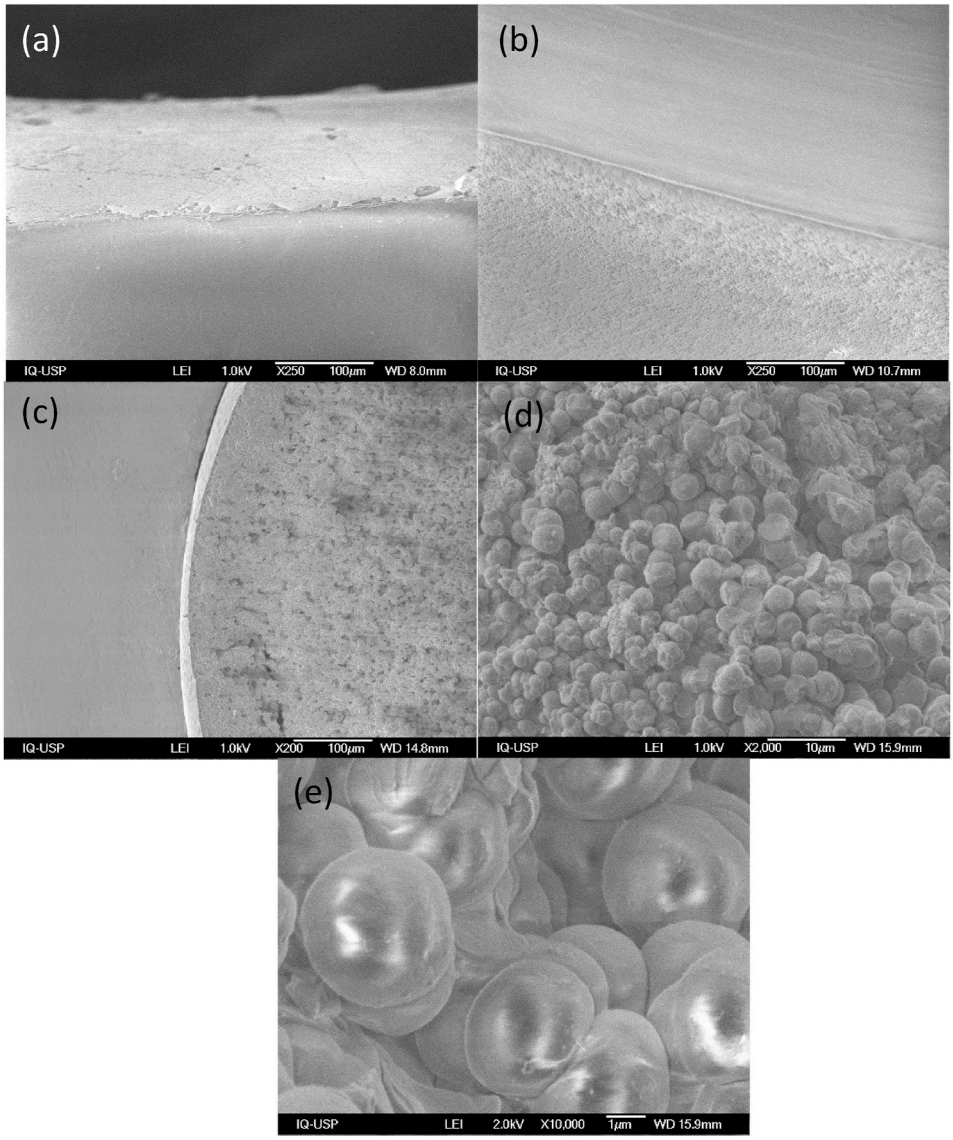

Fig. 2. SEM images of the internal surface of a longitudinally cut FEP tube before (a) and after (b) the photografting with BP and EDMA, the upper part of the figure showing the cut wall and the lower part the internal surface. Cross-section images show the poly(LMA-*co*-EDMA) monolith filling the tube (c) without gaps between the wall and the monolith. Globules of around 3 μm interconnected by the flow-through pores appear in (d) and (e) with different amplifications.

The chromatographic performance of the columns was tested in the separation of a mixture of four proteins by RPLC using a gradient of ACN in 0.10% (v/v) TFA (Fig. 3). Retention factors, selectivity, peak symmetry, and resolution (Table 1) show that the performance of the columns and the repeatability of the parameters are quite acceptable. From all chromatograms, it is possible to estimate resolutions > 1.8, that is, baseline separation for all the studied proteins. The retention factors were in the range $7 < k < 14$, denoting that under the gradient conditions, the reversed-phase mechanism firmly retained the proteins. The asymmetry factor was predominantly > 2, although some values as large as 3.1 were observed for ribonuclease A in columns 3 and 4, but not confirmed for columns 1, 2 and 5, for which the asymmetry factors were acceptable. Additional data on the reproducibility of peak areas and retention times observed in the five columns appear in Table S1.

One of the columns was used to make a test of repeatability of separation in two different days separated by a 15-days interval, during which the columns were stored in ACN or applied to real egg white samples (Fig. S2). The RSD of the retention times in intraday experiments was between 0.045 and 0.29%, whereas the RSD was within the 0.27–0.39% range in the interday tests (Fig. S3). The RSD of peak areas in intraday experiments was between 1.34 (lysozyme) and 11.8% (ovalbumin). In the interday experiment, the RSD of peak areas varied from 3.86 (myoglobin) to 19.8% (ovalbumin) (Fig. S3). The most significant variation observed in both intraday and interday experiments for ovalbumin is not clear. The systematic decrease of peak area from the first to the second experiment day is probably caused by the degradation of the protein under storage in the refrigerator during the 15 days.

3.4. Application to real samples

3.4.1. Application to egg white

The chromatogram of the egg white sample diluted 1:10 (v/v) in 0.010 mol L^{-1} PBS shows nine peaks (Fig. 4). Spiking this sample with a 1.0 mg mL^{-1} mixture of lysozyme and ovalbumin revealed that peak 3 is due to lysozyme (Fig. 4a). The concentration of ovalbumin is much larger than that of lysozyme. Consequently, in this first experiment, it was not possible to observe any variation in the peak of ovalbumin. Then, the sample solution was diluted 1:500 in PBS and analyzed again, before and after spiking with the mixture of 1.0 mg mL^{-1} of the two

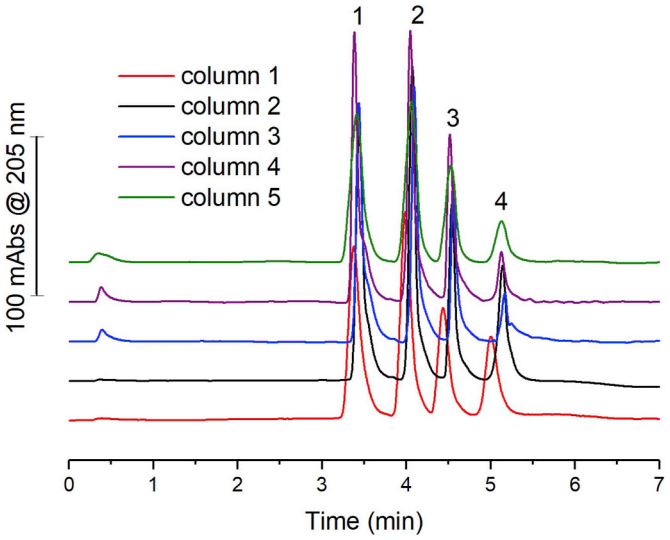

Fig. 3. Blank subtracted chromatograms showing the separation of (1) ribonuclease A, (2) lysozyme, (3) myoglobin, and (4) ovalbumin by reversed-phase liquid chromatography on five poly(LMA-co-EDMA) columns using a gradient of 5–70% (v/v) ACN in 0.10% (v/v) TFA in 5 min, isocratic at 70% ACN until 7 mn. Flow rate = 500 μL min^{-1}, Temperature = 60 °C, Sample volume = 2 μL. All proteins at concentration 1.0 mg mL^{-1}.

proteins (Fig. 4b). The complete chromatograms of the samples superposed to the blank appear in the Supplementary Information (Fig. S4). This experiment enabled the visualization of the increment of peaks 3 and 8 after the spiking, thus allowing the assignment of peak 8 to ovalbumin. The elution order is consistent with those described in previous works using RPLC [29,30], as well as with the number of chromatographic peaks observed for other egg white samples. It is noteworthy that the recovery of ovalbumin approaches 100% in this poly(LMA-*co*-EDMA) column, even from very concentrated solutions (Fig. 4a). Analysis of egg white with C_4 or C_{18} bonded silica-based particulate stationary phases required several blank runs to achieve the total recovery of ovalbumin [29,31].

The retention times of lysozyme and ovalbumin in the egg white sample were indistinguishable from those observed in the mix of purified proteins (Fig. 3 or Fig. S4). Hence, to quantify the proteins, an external calibration curve was prepared in a concentration range between 0.050 and 1.0 mg mL^{-1}. The statistical parameters of the calibration curves are summarized in Table 2, denoting excellent linearity, as well as suitable detectability. The concentrations of lysozyme and ovalbumin were 0.93 and 47 mg mL^{-1}, respectively. From the spiking experiments, it was possible to estimate recoveries of 83% for lysozyme and 103% for ovalbumin, demonstrating the acceptable accuracy of the analysis.

3.4.2. Myoglobin in urine

Urinary myoglobin is a marker of muscle damage, used to assess the severity of injury and recovery of patients of myocardial infarcts, traumas, as well as intense physical exercises [26]. Quantitative analysis has been made by sensitive but expensive methodologies such as immunoassays, histochemical staining, radioimmunoassay, among others. Liquid chromatography with UV–Vis detection is a robust, low-cost alternative to these methods, as demonstrated, for instance, by Lyndsay et al. [26].

In the present work, the poly(LMA-*co*-EDMA) column was used to investigate the presence of myoglobin in urine samples from one of the co-authors, collected before and after physical exercises. Before the activities, the chromatogram of the sample diluted (1:4) in 10 mmol L^{-1} PBS had no detectable proteins. The peak of unretained compounds (Fig. 5 and Fig. S5) is due to the buffer itself, salts, and small polar molecules. The sample collected after physical exercises exhibited a measurable myoglobin peak, confirmed by spiking the sample with 0.50 mg mL^{-1} of the protein (Fig. 5). The retention time at 4.38 min was consistent with the previous studies in pure water (Fig. 3 and Fig. S2).

An external calibration curve constructed with 0.050–1.0 mg mL^{-1} myoglobin solutions (Table 2) was used to estimate a concentration of 36 μg mL^{-1} of myoglobin in the sample collected after the training. This result is consistent with the values between 0.19 and 63.3 μg mL^{-1} found by Lindsay et al. in the urine samples of 14 subjects following the training session [26]. The analyses of the urine samples (before training) spiked with 50, 100, 200, and 400 μg mL^{-1} resulted in recoveries of 112, 110, 82, and 106%, respectively, denoting a good accuracy for the analysis of this real sample.

It is noteworthy that, excepting the peak of unretained compounds, there are no other significant peaks in the chromatograms of samples collected before the training session. In the sample collected after the training, additionally to the myoglobin peak, another measurable peak, baseline resolved to myoglobin, was observed at 4.17 min. The total chromatographic run lasts only 12 min, including the reconditioning step (Fig. S5). The RPLC method proposed by Lyndsay et al. [26] used a similar gradient in a 5-μm, 150 × 4.6 mm column at the flow rate of 1.0 mL min^{-1}, requiring a run time of 32 min, with myoglobin eluting at about 15 min, preceded by several other peaks that were not observed in the chromatograms obtained in the monolithic column. These peaks are probably due to small molecules that were retained in the particulate columns, but not in the polymer monolith, thus demonstrating an overwhelming advantage of these columns for determination/purification of proteins in samples rich in small molecules.

4. Conclusion

In this work, 1.57 mm i.d. FEP tubes were easily functionalized to serve as molds for monolithic columns, thus being an alternative to ETFE, PP, fused silica, and PEEK tubes in narrow bore chromatography.

Table 1
Chromatographic parameters for reversed-phase separation of proteins on the poly(LMA-co-EDMA) columns.

Protein	Column 1				Column 2				Column 3				Column 4				Column 5			
	K[a]	α	Asy[b]	Rs[c]	K	α	Asy	Rs	K	α	Asy	Rs	K	α	Asy	Rs	K	α	Asy	Rs
RnaseA	7.41	–	1.80	–	7.51	–	2.42	–	7.51	–	3.0	–	7.70	–	3.1	–	9.1	–	1.35	–
Lysozyme	8.89	1.20	2.05	2.54	9.12	1.21	1.41	4.59	9.17	1.22	2.33	5.01	9.41	1.22	1.88	5.65	11.1	1.22	1.25	2.64
Myoglobin	9.97	1.12	1.82	1.80	10.3	1.13	2.00	3.70	10.3	1.12	1.8	4.02	10.6	1.12	2.5	3.46	12.5	1.12	1.02	1.92
Ovalbumin	11.4	1.14	1.71	2.27	11.7	1.14	1.72	4.30	11.8	1.14	2.50	6.14	12.2	1.15	2.13	4.30	14.2	1.13	2.20	2.57

[a] retention factor: $K = \frac{t_R - t_0}{t_0}$, where t_R is the retention time and t_0 is the retention time of the unretained solvent.

[b] Asymmetry – computed a 10% of peak height.

[c] Resolution - $Rs = \frac{1.18(t_2 - t_1)}{\left(W_{\frac{1}{2},1} + W_{\frac{1}{2},2}\right)}$, where t_2 and t_1 are the retention times of 2 and 1, and $W_{\frac{1}{2},1}$ and $W_{\frac{1}{2},2}$ are the peak width at half height.

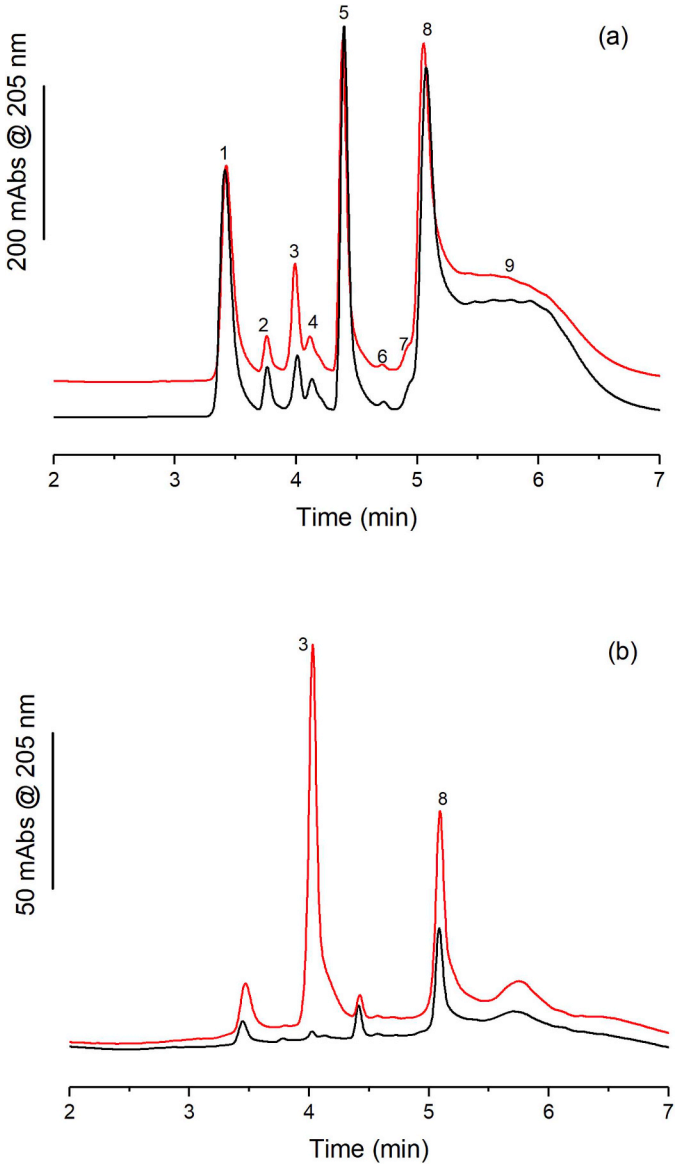

Fig. 4. (a) Blank subtracted chromatograms of egg white samples diluted at 1:10 ratio (v/v) in 0.050 mol L^{-1} PBS (pH 7.0) before (black) and after (red) spiking the sample (900 μL) with 100 μL of 1.0 mg mL^{-1} mixture of lysozyme (peak 3) and ovalbumin (peak 8), and (b) the same as (a) but after diluting the sample at 1:500 ratio in PBS. Chromatographic conditions are the same as in the caption of Fig. 3. (For interpretation of the references to colour in this figure legend, the reader is referred to the Web version of this article.)

The grafting of the poly(EDMA) thin layer on the surface of the FEP rendered enough density of vinyl functionalities to covalently attach poly(LMA-co-EDMA) monolith. Low RSD of the permeabilities demonstrated the excellent repeatability of five columns prepared in two different days. The columns exhibited excellent performance in the separation of proteins, being stable for several working days under flow rates of 500 μL min^{-1} in gradients of 5–70% (v/v) ACN in 0.1% TFA and pressures $<$ 400 psi. Analysis of real samples provided excellent recoveries of ovalbumin and lysozyme (egg white) and myoglobin (urine).

CRediT authorship contribution statement

Fernando H. do Nascimento: Conceptualization, Methodology, Investigation. **Amanda H. Moraes:** Investigation, Formal analysis. **Catharina R.L. Trazzi:** Investigation. **Caryna M. Velasques:**

Table 2
Retention times, calibration parameters for a concentration range between 0.050 and 1.0 mg mL^{-1}, and detectability of the method.

Protein	t_R (min)	Slope (mAbs min mL mg^{-1})	Intercept (mAbs. min)	R^2	LOD[a] (μg mL^{-1})	LOQ[a] (μg mL^{-1})
Lysozyme	4.03 ± 0.02	65.9 ± 0.6	−2.0 ± 0.3	0.999	3.0	9.9
Ovalbumin	5.11 ± 0.01	21.8 ± 0.7	−0.1 ± 0.4	0.997	7.9	26
Myoglobin	4.37 ± 0.02	38 ± 2	−0.4 ± 0.7	0.994	4.2	13.9

[a] LOD and LOQ were computed at the 3 and 10:1 signal-to-noise ratio, respectively.

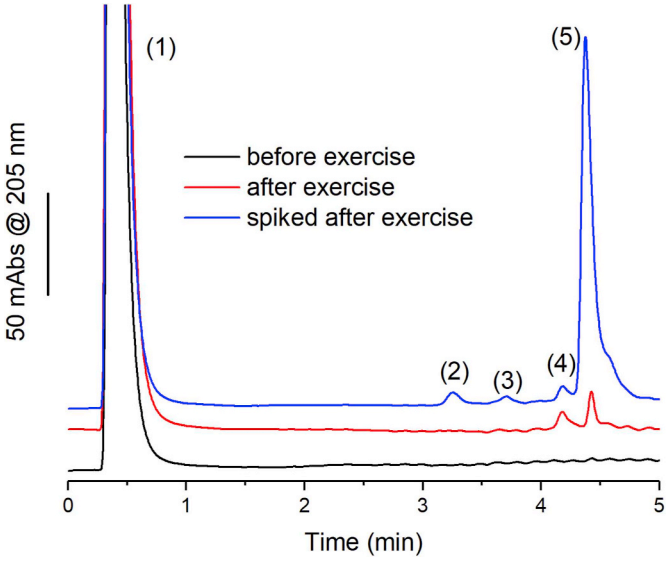

Fig. 5. Blank subtracted chromatograms of urine samples diluted 1:4 (v/v) in 10 mmol L^{-1} PBS (pH 7.0) collected before and after physical exercises, (1) unretained compounds, (2) and (3) myoglobin impurities, (4) unknown protein, (5) myoglobin. Spike was made at the 500 μg mL^{-1} concentration. Chromatographic conditions: gradient of 5–70% (v/v) ACN in 0.10% (v/v) TFA in 5 min, isocratic at 70% ACN until 7 mn. Flow rate = 500 μL min^{-1}, Temperature = 60 °C, Sample volume = 2 μL.

Investigation. **Jorge C. Masini:** Supervision, Writing - review & editing.

Declaration of competing interest

The authors declare that there are no competing interests.

Acknowledgments

This work was funded by grants 2013/18507-4 from the São Paulo Research Foundation (FAPESP) and 303940/2017-4 from the National Council for Scientific and Technological Development (CNPq). FHN acknowledges Coordination for the Improvement of Higher Education Personnel (CAPES) for a post-doc fellowship (Contract 88882.315696/2019–01). CRLT acknowledges CNPq for a Scientific Initiation fellowship (120615/2019-3)

Appendix A. Supplementary data

Supplementary data to this article can be found online at https://doi.org/10.1016/j.talanta.2020.121063.

References

[1] U. Andjelković, S. Tufegdžić, M. Popović, Use of monolithic supports for high-throughput protein and peptide separation in proteomics, Electrophoresis 38 (2017) 2851–2869, https://doi.org/10.1002/elps.201700260.
[2] M. Rigobello-Masini, J.C.P. Penteado, J.C. Masini, Monolithic columns in plant proteomics and metabolomics, Anal. Bioanal. Chem. 405 (2013) 2107–2122, https://doi.org/10.1007/s00216-012-6574-6.
[3] K.B. Lynch, J. Ren, M.A. Beckner, C. He, S. Liu, Monolith columns for liquid chromatographic separations of intact proteins: a review of recent advances and applications, Anal. Chim. Acta 1046 (2019) 48–68, https://doi.org/10.1016/j.aca.2018.09.021.
[4] X. Han, Y. Xie, Q. Wu, S. Wu, The effect of monolith properties on the digestion performance of monolith-based immobilized enzyme microreactor, J. Chromatogr. Sci. 57 (2019) 116–121, https://doi.org/10.1093/chromsci/bmy091.
[5] M. Naldi, U. Černigoj, A. Štrancar, M. Bartolini, Towards automation in protein digestion: Development of a monolithic trypsin immobilized reactor for highly efficient on-line digestion and analysis, Talanta 167 (2017) 143–157, https://doi.org/10.1016/j.talanta.2017.02.016.
[6] Q.C. Wang, F. Svec, J.M.J. Fréchet, Macroporous polymeric stationary-phase rod as continuous separation medium for reversed-phase chromatography, Anal. Chem. 65 (1993) 2243–2248, https://doi.org/10.1021/ac00065a013.
[7] G. Desmet, S. Eeltink, Fundamentals for LC miniaturization, Anal. Chem. 85 (2013) 543–556, https://doi.org/10.1021/ac303317c.
[8] E. Vasconcelos Soares Maciel, A.L. de Toffoli, E. Sobieski, C.E. Domingues Nazário, F.M. Lanças, Miniaturized liquid chromatography focusing on analytical columns and mass spectrometry: a review, Anal. Chim. Acta (2019), https://doi.org/10.1016/j.aca.2019.12.064.
[9] F. Svec, Y. Lv, Advances and recent trends in the field of monolithic columns for chromatography, Anal. Chem. 87 (2015) 250–273, https://doi.org/10.1021/ac504059c.
[10] M.R. Gama, F.R.P. Rocha, C.B.G. Bottoli, Monoliths: synthetic routes, functionalization and innovative analytical applications, TrAC Trends Anal. Chem. (Reference Ed.) 115 (2019) 39–51, https://doi.org/10.1016/j.trac.2019.03.020.
[11] J.C. Masini, Semi-micro reversed-phase liquid chromatography for the separation of alkyl benzenes and proteins exploiting methacrylate- and polystyrene-based monolithic columns, J. Separ. Sci. 39 (2016) 1648–1655, https://doi.org/10.1002/jssc.201600049.
[12] S. Shu, H. Kobayashi, M. Okubo, A. Sabarudin, M. Butsugan, T. Umemura, Chemical anchoring of lauryl methacrylate-based reversed phase monolith to 1/16' o.d. polyetheretherketone tubing, J. Chromatogr., A 1242 (2012) 59–66, https://doi.org/10.1016/j.chroma.2012.04.030.
[13] S. Eeltink, S. Dolman, F. Detobel, G. Desmet, R. Swart, M. Ursem, 1 mm ID poly (styrene-co-divinylbenzene) monolithic columns for high-peak capacity one- and two-dimensional liquid chromatographic separations of intact proteins, J. Separ. Sci. 32 (2009) 2504–2509, https://doi.org/10.1002/jssc.200900068.
[14] S. Shu, H. Kobayashi, N. Kojima, A. Sabarudin, T. Umemura, Preparation and characterization of lauryl methacrylate-based monolithic microbore column for reversed-phase liquid chromatography, J. Chromatogr., A 1218 (2011) 5228–5234, https://doi.org/10.1016/j.chroma.2011.05.104.
[15] J.C. Masini, Separation of proteins by cation-exchange sequential injection chromatography using a polymeric monolithic column, Anal. Bioanal. Chem. 408 (2016) 1445–1452, https://doi.org/10.1007/s00216-015-9242-9.
[16] M. Iacono, D. Connolly, A. Heise, Fabrication of a GMA-co-EDMA monolith in a 2.0 mm i.d. Polypropylene housing, Materials 9 (2016) 263, https://doi.org/10.3390/ma9040263.
[17] M. Catalá-Icardo, S. Torres-Cartas, S. Meseguer-Lloret, E.F. Simó-Alfonso, J.M. Herrero-Martínez, Photografted fluoropolymers as novel chromatographic supports for polymeric monolithic stationary phases, Talanta 187 (2018) 216–222, https://doi.org/10.1016/j.talanta.2018.05.026.
[18] M. Catalá-Icardo, S. Torres-Cartas, E.F. Simó-Alfonso, J.M. Herrero-Martínez, Influence of photo-initiators in the preparation of methacrylate monoliths into poly (ethylene-co-tetrafluoroethylene) tubing for microbore HPLC, Anal. Chim. Acta 1093 (2020) 160–167, https://doi.org/10.1016/j.aca.2019.09.055.
[19] A. Namera, T. Saito, Advances in monolithic materials for sample preparation in drug and pharmaceutical analysis, Trends Anal. Chem. 45 (2013) 182–196, https://doi.org/10.1016/j.trac.2012.10.017.
[20] J.C. Masini, F. Svec, Porous monoliths for on-line sample preparation: a review, Anal. Chim. Acta 964 (2017) 24–44, https://doi.org/10.1016/j.aca.2017.02.002.
[21] T.B. Stachowiak, T. Rohr, E.F. Hilder, D.S. Peterson, M. Yi, F. Svec, J.M.J. Fréchet, E.O.L. Berkeley, Fabrication of Porous Polymer Monoliths Covalently Attached to the Walls of Channels in Plastic Microdevices, (2003), pp. 3689–3693, https://doi.org/10.1002/elps.200305536.
[22] H. Wang, H. Zhang, Y. Lv, F. Svec, T. Tan, Polymer monoliths with chelating functionalities for solid phase extraction of metal ions from water, J. Chromatogr., A 1343 (2014) 128–134, https://doi.org/10.1016/j.chroma.2014.03.072.
[23] I. Noh, K. Chittur, S.L. Goodman, J.A. Hubbell, Surface modification of poly (tetrafluoroethylene) with benzophenone and sodium hydride, J. Polym. Chem. - Part A, Polym. Chem. 35 (1997) 1499–1514.
[24] S. Eeltink, L. Geiser, F. Svec, J.M.J. Fréchet, Optimization of the porous structure and polarity of polymethacrylate-based monolithc capillary columns for the LC-MS separation of enzymatic digests, J. Separ. Sci. 30 (2007) 2814–2820, https://doi.org/10.1002/jssc.200700185.
[25] X. Wang, X. Li, X. Jiang, P. Dong, H. Liu, L. Bai, H. Yan, Preparation of a poly (styrene-co-DPHA-co-EDMA) monolith and its application for the separation of small molecules and biomacromolecules by HPLC, Talanta 165 (2017) 339–345, https://doi.org/10.1016/j.talanta.2016.12.071.
[26] A. Lindsay, S. Carr, N. Draper, S.P. Gieseg, Urinary myoglobin quantification by high-performance liquid chromatography: an alternative measurement for exercise-induced muscle damage, Anal. Biochem. 491 (2015) 37–42, https://doi.org/10.1016/j.ab.2015.09.001.
[27] A. Forner-Cuenca, V. Manzi-Orezzoli, J. Biesdorf, M. El Kazzi, D. Streich, L. Gubler, T.J. Schmidt, P. Boillat, Advanced water management in PEFCs: diffusion layers with patterned wettability: I. Synthetic routes, wettability tuning and thermal stability, J. Electrochem. Soc. 163 (2016) F788–F801, https://doi.org/10.1149/2.0271608jes.
[28] R.M. Abdul Majeed, V.S. Purohit, S.V. Bhoraskar, A.B. Mandale, V.N. Bhoraskar, Irradiation effects of 12 eV oxygen ions on polyimide and fluorinated ethylene propylene, Radiat. Eff. Defect Solid 161 (2006) 495–503, https://doi.org/10.1080/10420150600810224.
[29] A.C. Awadé, T. Efstathiou, Comparison of three liquid chromatographic methods for egg-white protein analysis, J. Chromatogr. B Biomed. Sci. Appl. 723 (1999) 69–74, https://doi.org/10.1016/S0378-4347(98)00538-6.
[30] F. Nau, A. Mallard, J. Pages, G. Brulé, Reversed-phase liquid chromatography of egg white proteins. Optimization of ovalbumin elution, J. Liq. Chromatogr. Relat. Technol. 22 (1999) 1129–1147, https://doi.org/10.1081/JLC-100101722.
[31] H. Itoh, N. Nimura, T. Kinoshita, N. Nagae, M. Nomura, Fast protein separation by reversed-phase high-performance liquid chromatography on octadecylsilyl-bonded nonporous silica gel. II. Improvement in recovery of hydrophobic proteins, Anal. Biochem. 199 (1991) 7, https://doi.org/10.1016/0003-2697(91)90261-Q.